Three-Dimensional Quantitative Structure−Activity Relationship of Interleukin 1-β Converting Enzyme Inhibitors: A Comparative Molecular Field Analysis Study

Santosh S. Kulkarni and Vithal M. Kulkarni*

Department of Chemical Technology, Pharmaceutical Division, University of Mumbai, Matunga, Mumbai 400 019, India

Received December 15, 1997

A three-dimensional quantitative structure−activity relationship (QSAR) study using the comparative molecular field analysis (CoMFA) method was performed on a series of interleukin 1-β converting enzyme (ICE) inhibitors. The compounds studied have been reported to be time-dependent inhibitors of ICE. This study was performed using 49 compounds, in which the CoMFA models were developed using a training set of 39 compounds. All the compounds were modeled using the X-ray crystal structure of tetrapeptide aldehyde inhibitor/ICE complex. The inhibitor compounds were considered both as neutral species and as P1 carboxylate ionized species. Superimpositions were performed using two alignment rules, namely, an alignment of the structures based on RMS fitting of the backbone heavy atoms of each structure to compound **2** and an alignment based on SYBYL QSAR rigid body field fit of the steric and electrostatic fields of the molecules to the fields of compound **2**. Use of LUMO energies or ClogP as additional descriptors in the QSAR table did not improve the significance of the CoMFA models. Steric and electrostatic fields of the inhibitors were found to be the relevant descriptors for structure−activity relationships. The predictive ability of the CoMFA model was evaluated by using a test set of 10 compounds (r^2_{pred} as high as 0.859). Further comparison of the coefficient contour maps with the steric and electrostatic properties of the receptor show a high level of compatibility.

Introduction

Human interleukin 1-β converting enzyme (ICE) is a processing cysteine protease involved in the production of inflammatory mediator interleukin 1-β (IL-1β).[1−3] ICE is located primarily in monocytes and specifically cleaves the biologically inactive 31 kDa precursor interleukin 1β (ProIL-1β) at the sequence-related site Asp27-Gly28 and Asp116-Ala117 to produce the 17.5 kDa biologically active inflammatory cytokine IL-1β.[4] IL-1β has been implicated in pathophysiology of many inflammatory and autoimmune diseases, including septic shock, rheumatoid arthritis, inflammatory bowel disease, and insulin-dependent diabetes mellitus.[5] Some observations have suggested that apoptosis[6,7] (programmed cell death) as observed in degenerative neuronal diseases such as Alzheimer's and Parkinson's disease may be regulated by ICE or a related enzyme.[8] Development of inhibitors of ICE provide a new therapeutic approach for the treatment of inflammatory diseases and other diseases that arise from excessive or premature cell death.

ICE has a substrate specificity[9] in which it has a requirement of aspartic acid at the P1 position for effective catalysis. Using the substrate specificity data, several potent reversible inhibitors of ICE have been designed.[10,11] Tetrapeptide aldehyde is a potent, reversible, transition state inhibitor of ICE.[3] Krantz and Smith[12] have described peptide (acyloxy) methyl ketones as potent, selective inactivators of cysteine protease. These inhibitors contain a reactive group (leaving group) or an atom vulnerable to S_N2 displacements attached to a recognition site (Figure 1) characteristic of the substrate. Recently ICE inhibitors containing acyloxy methyl ketones,[13,14] α-((1-phenyl 3-(trifluoromethyl)-pyrazol-5-yl)oxy)methyl ketones,[15] and α,α-((diphenylphosphin)-oxy)methyl ketones[16] as leaving groups have been reported. These inhibitors first bind to the ICE active site noncovalently, and then the inactivation proceeds through expulsion of the carboxylate leaving group to form a thiomethyl ketone with the active site Cys 285. Structure−activity data generated so far suggest that the potency of these inhibitors is related to the extent of noncovalent interactions rather than its vulnerability to undergo S_N2 displacement. Therefore the reactivity of the inhibitors alone cannot explain the efficiency of inhibition. The intermolecular noncovalent interactions of the nonreacting parts of the inhibitor and the enzyme may contribute toward enzyme affinity. To gain further insight into the relationship between the structure and biological activity, we have applied a three-dimensional quantitative structure−activity relationship (QSAR) approach comparative molecular field analysis (CoMFA).[17,18]

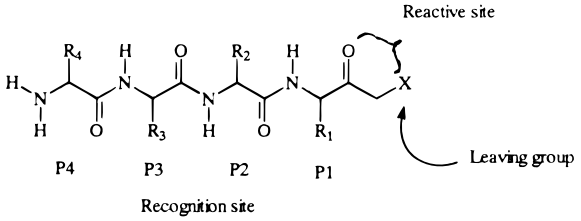

Figure 1. General structure of ICE inhibitors.

CoMFA was introduced in 1988 by Cramer.[17,18] In this method a relationship is established between the

10.1021/jm9708442 CCC: $18.00 © 1999 American Chemical Society
Published on Web 01/27/1999

biological activities of a set of compounds and their steric and electrostatic properties. An "active conformation" of the ligands are generated and superimposed according to predefined rules. These molecules are then placed in a box of predefined grid size. The steric and electrostatic interaction energy between each structure and a probe atom of defined size and charge are calculated at each grid point using the molecular mechanics force fields. A multivariate data analysis technique called partial least squares (PLS)[19,20] was used to derive linear equations from the resulting matrices. PLS was used in combination with cross-validation to obtain the optimum number of components (latent variables). This ensures that the QSAR models were selected based on their ability to predict the data rather than to fit the data. The advantages of the CoMFA studies are in the ability to predict the target properties of the compounds and to graphically present the QSAR in the form of coefficient contour maps. The identification of the bioactive conformation of the ligands under investigation is one of the crucial steps in CoMFA. Various successful examples of CoMFA studies on conformationally constrained small molecules have been reported including steroids,[17,21] clodronic acid esters,[22] flavones,[23] angiotensin-converting enzyme inhibitors,[24,25] pyrazoloacridines,[26] polyhalogenated dibenzo-p-dioxins, dibenzofurans, biphenyls,[27] and acetyl cholinesterase inhibitors.[28,29] The bioactive conformation of the conformationally flexible ligands can be obtained from X-ray crystallographic and NMR studies. The use of such structural data in a CoMFA study have been reported for human immunodeficiency virus-1 protease,[30] human rhinovirus-14,[31] thermolysin, renin,[32] and protein tyrosine kinase[33] inhibitors.

In this paper we present a study of CoMFA of ICE inhibitors. Since no NMR or X-ray crystallographic data on the conformations of these inhibitors were available, we have employed the X-ray crystallographic data of tetrapeptide aldehyde inhibitor bound to ICE[34] for molecular modeling of these inhibitors. CoMFA was applied to rationalize the relationship between ICE inhibitor structures and their activities. Thus it is hoped that CoMFA can help to describe the important structural features essential for enhancing the biological activity that can be used to design new ICE inhibitors.

Methods

Biological Data. We have selected 49 diverse inhibitors of ICE whose activity was expressed as second-order rate constant for inactivation.[13−16,35] These kinetic constants were measured by two research groups. Both authors have used similar methods to determine ICE inhibitory activity. [13,14] The enzyme used in these assays was obtained from same source, monocytic THP-1 cell line. The error in the measurement of rate constant was below 10%. The logarithm of the measured rate of inactivation was used in CoMFA, thus correlating the data linearly to the free energy change. The structures of 49 compounds used in the present study are tabulated in Tables 1−3. These inhibitors included 2 tetrapeptides, 17 tripeptides, 10 dipeptides, 9 monopeptides, and 11 peptidomimetic[35] inhibitors. It is essential to assess the predictive power of models by using a test set of compounds. This was achieved by arbitrarily setting aside 10 compounds as a test set (test set 1) with a regularly distributed biological data. The mean (standard deviation) of the biological activity of the training and test set was 4.48 (1.23) and 4.44 (1.28), respectively.

Molecular Modeling. Molecular modeling and CoMFA studies were performed on a Silicon Graphics INDY R5000 computer. Structural manipulations were performed with molecular modeling package SYBYL 6.22[36] using the standard TRIPOS force field.[37] Partial atomic charges of ligands were calculated using the AM1 model Hamiltonian[38] within MOPAC 6.0[39] (keywords 1SCF, MMOK). (Coordinates of all the molecules in Sybyl mol2 format are available from the authors upon request; email, vishalk@giasbmc.vsnl.net.in.)

Table 1. Structures and Measured Activities of the Peptidic ICE Inhibitors Used as Training Set

compd	structure	biological[a] activity	ref
1	Ac-Tyr-Val-Ala-Asp-$CH_2OC(O)$-[2,6$(CF_3)_2$]Ph	5.98	13
2	Ac-Tyr-Val-Ala-Asp-$CH_2OC(O)$-[2,6$(CH_3)_2$]Ph	6.04	13
3	Ph$(CH_2)_2$C(O)-Val-Ala-Asp-$CH_2OC(O)$-[2,6$(CF_3)_2$]Ph	5.95	13
4	Ph$(CH_2)_2$C(O)-Val-Ala-Asp-$CH_2OC(O)$-[2,6$(OH)_2$]Ph	5.85	13
5	Ph$(CH_2)_2$C(O)-Val-Ala-Asp-$CH_2OC(O)$-Ph	5.45	13
6	Ph$(CH_2)_2$C(O)-Val-Ala-Asp-$CH_2OC(O)$-[2,3,4,5,6$(F)_5$]Ph	6.04	13
7	Ph$(CH_2)_2$C(O)-Val-Ala-Asp-$CH_2OC(O)$-[4-NO_2]Ph	6.11	13
8	Alloc-Asp-$CH_2OC(O)$-[2,6$(CF_3)_2$]Ph	3.72	13
9	Alloc-Asp-$CH_2OC(O)$-[2,6$(OH)_2$]Ph	3.43	13
10	Alloc-Asp-$CH_2OC(O)$-[2,6(CH_3)2]Ph	2.91	13
11	Alloc-Asp-$CH_2OC(O)$-[2,3,4,5,6$(F)_5$]Ph	2.99	13
12	Alloc-Asp-$CH_2OC(O)$-[4-NO_2]Ph	1.79	13
13	Z[b]-Asp-CH_2-DCB[c]	3.85	14
14	Z-Val-Asp-CH_2-DCB	4.61	14
15	Z-Val-Ala-Asp-CH_2-DCB	5.61	14
16	Z-Asp-CH_2-PTP[d]	4.04	15
17	Z-Phe-Ala-CH_2-PTP	2.70	15
18	Z-Val-Asp-CH_2-PTP	4.30	15
19	Z-Val-Ala-N(Me)Asp-CH_2-PTP	2.48	15
20	Z-Val-N(Me)Ala-Asp-CH_2-PTP	5.37	15
21	Z-Val-Pro-Asp-CH_2-PTP	5.06	15
22	Z-Val-Pip-Asp-CH_2-PTP	5.43	15
23	Z-Pro-Val-Asp-CH_2-PTP	2.48	15
24	Z-Asp-CH_2-DPP[e]	4.07	16
25	Z-Val-Asp-CH_2-DPP	4.70	16
26	Z-Val-Asp-CH_2-HPP[f]	2.70	16
27	Z-Val-Asp-CH_2-DCPP[g]	4.89	16
28	Z-Val-Ala-Asp-CH_2-DCPP	5.36	16
29	Z-Phe-Ala-CH_2-DPP	2.70	16
30	Z-Leu-Phe-CH_2-DPP	2.70	16

[a] Expressed as the logarithm of the second-order rate constant for inactivation. [b] Z = benzyloxycarbonyl. [c] DCB = (2,6-dichlorobenzoyl)oxy. [d] PTP = (1-phenyl-3-(trifluoromethyl)pyrazol-5-yl)oxy. [e] DPP = (diphenylphosphinyl)oxy. [f] HPP = (phenylphosphinyl)oxy. [g] DCPP = (bis(4-chlorophenyl)phosphinyl)oxy.

Table 2. Structures and Measured Activities of the Peptidomimetic ICE Inhibitors Containing 5-Amino Pyrimidin-6-one System Used as Training and Test Sets

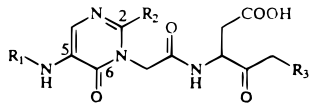

compd	R_1	R_2	R_3	biological[a] activity	ref
31[b]	Z[d]	4-FPh	PTP[e]	5.20	35
32[b]	Z	4-FPh	DPP[f]	5.16	35
33[b]	Z	2-thienyl	DCB[g]	5.43	35
34[b]	Z	3-pyridinyl	PTP	5.16	35
35[b]	$PhCH_2NHCO$	4-FPh	DCB	5.17	35
36[b]	(2-furanyl)CO	4-FPh	DCB	4.66	35
37[b]	$Me_2N(CH_2)_5CO$	4-FPh	DCB	4.95	35
38[b]	$PhSO_2$	4-FPh	DCB	4.95	35
39[b]	H	4-FPh	DCB	4.56	35
T9[c]	Z	4-FPh	DCB	5.43	35
T10[c]	Z	Me	PTP	4.98	35

[a] Expressed as the logarithm of the second-order rate constant for inactivation. [b] Member of the training set. [c] Member of the test set. [d] Z = benzyloxycarbonyl. [e] PTP = (1-phenyl-3-(trifluoromethyl)pyrazol-5-yl)oxy. [f] DPP = (diphenylphosphinyl)oxy. [g] DCB = (2,6-dichlorobenzoyl)oxy.

Table 3. Structures and Measured Activities of the Peptidic ICE Inhibitors Used as Test Set

compd	structure	biological[a] activity	ref
T1	Z[b]-Phe-Ala-CH_2-DCB[c]	2.70	16
T2	Ph$(CH_2)_2$C(O)-Val-Ala-Asp-CH_2-O-C(O)[2,6$(CH_3)_2$]Ph	6.08	13
T3	Alloc-Asp-CH_2-O-C(O)-Ph	2.00	13
T4	Z-Val-Ala-Asp-CH_2-PTP[d]	5.45	15
T5	Z-N(Me)Val-Ala-Asp-CH_2-PTP	3.93	15
T6	Z-Val-Aze-Asp-CH_2-PTP	4.66	15
T7	Z-Val-Ala-Asp-CH_2-DPP[e]	5.07	16
T8	Z-Val-Asp-CH_2-DMP[f]	4.09	16

[a] Expressed as the logarithm of the second-order rate constant for inactivation. [b] Z = benzyloxycarbonyl. [c] DCB = (2,6-dichlorobenzoyl)oxy. [d] PTP = (1-phenyl-3-(trifluoromethyl)pyrazol-5-yl)oxy. [e] DPP = (diphenylphosphinyl)oxy. [f] DMP = (dimethylphosphinyl)oxy.

The first CoMFA model (model A) was constructed in the neutral form based on the coordinates of the inhibitor taken from ICE/tetrapeptide aldehyde inhibitor complex (Protein Data Bank entry 1ICE) determined by X-ray crystallography.[34] The inhibitor was extracted and all hydrogens were added with standard geometries. Partial atomic charges were calculated for the tetrapeptide aldehyde inhibitor using the MOPAC/AM1 Hamiltonian. This structure was then optimized by energy minimization using the Broyden, Fletcher, Goldfarb, and Shannon (BFGS) algorithm to a final root-mean-square gradient of 0.01 kcal/mol. The default settings for all other minimization options and a distance-dependent dielectric function were employed throughout the calculation. All compounds were modeled by mutating the residues of tetrapeptide aldehyde. A constrained minimization was performed initially in which the unchanged residues of the new analogues were defined as an aggregate to constrain their conformation. The constraints were then removed, and the minimization was repeated till the root-mean-square convergence reached to 0.01 kcal/mol Å. In our earlier studies we have performed the docking analysis of some ICE inhibitors.[40] We have compared the conformations of these ligands with those obtained from the docking studies. A low root mean square deviation (RMSD) between the heavy atoms of the ligands supports our choice of the conformations obtained from the mutation technique for the CoMFA studies.

Model A was based on the neutral ligands. The P1 carboxylate of the inhibitors is essential for the recognition at the active site of ICE.[41] It is likely that this carboxylate group can get ionized under assay conditions. Hence, to evaluate the CoMFA with respect to changes in electronic nature of the ligands we have developed model B. In this model all the inhibitors containing P1 aspartic acid residue were ionized, and partial atomic charges were assigned from open shell AM1 1SCF calculations with a charge of −1 on the system.

Alignment Rule. The alignment rule, i.e., molecular conformation and orientation, is one of the most sensitive input areas for CoMFA studies. In the present study two different alignment rules were adopted.

Alignment I: This alignment involved RMS fitting of the backbone heavy atoms of the ligands. The compounds were fitted to the active analogue compound **2** using the α-carbon, carbonyl carbon, and amide nitrogen atoms. Analogues which do not have a formal α-carbon atom such as peptidomimetics were fitted by choosing the carbon atom of the acetamido side chain. This alignment maximizes the overlap of the backbone heavy atoms of all the ligands.

Alignment II: The SYBYL QSAR rigid body field fit command was used for this alignment. Field fit uses a Simplex algorithm in SYBYL that minimizes the differences in steric and electrostatic fields averaged over all the lattice grid points to find the best fit. One of the most active compounds, **2**, was used as a reference compound. The more extensive fields ensured by the size and bulky pendant groups of compound **2** facilitated the rigid body field fit. This fit is dependent on the similarity and initial orientations of the molecules. Therefore all the molecules were first prealigned by backbone atoms (alignment I) before being fitted to the fields of the reference compound to reduce the multiple local minima problem.[42]

CoMFA Interaction Energies. The steric and electrostatic potential fields were calculated at each lattice intersection of a regularly spaced grid of 2.0 Å. The CoMFA region was defined automatically, and it extended past the van der Waal's volume of all the molecules in *X*, *Y*, and *Z* directions. The van der Waals (Lennard-Jones, 6−12) potential and coloumbic term which represent, respectively, steric and electrostatic fields were calculated using the TRIPOS force field. A distance-dependent dielectric expression $\epsilon = \epsilon o Rij$ with $\epsilon o = 1.0$ was used. An sp^3 carbon atom with a van der Waals radius of 1.52 Å and a +1.0 charge served as the probe atom to calculate steric and electrostatic fields. The steric and electrostatic contributions were truncated to ±30 kcal/mol, and the electrostatic contributions were ignored at lattice intersections with maximal steric interactions.

PLS Analysis. The partial least squares algorithm was used in conjugation with the cross-validation (leave-one-out) option to obtain the optimum number of components which was used to generate the final CoMFA model without cross-validation. The result from a cross-validated analysis was expressed as r^2_{cv}, which is defined as

$$r^2_{cv} = 1 - \text{PRESS}/\sum (Y - Y_{mean})^2$$

where $\text{PRESS} = \sum (Y - Y_{Pred})^2$.

The r^2_{cv} can take up values in the range from 1, suggesting a perfect model, to less than 0, where the errors of prediction are greater than the error from assigning each compound mean activity of the model. Cross-validated PLS analysis using the leave-one-out procedure employed 10 components, in which each compound is systematically excluded from the set and its activity was predicted by a model derived from the rest of the compounds. Thus cross-validation by the leave-one-out method evaluates the model not by how it best fits the data but by how it best predicts the data. The optimum number of components was defined as that which yielded the highest cross-validated r^2 value, which normally had the smallest RMS error of prediction (SEP). Equal weights were assigned to the steric and electrostatic descriptors using the CoMFA_STD scaling option. To speed up the analysis and reduce the amount of noise, a minimum σ (column filter) value of 2.0 kcal/mol was used. The final PLS analysis was then performed using the optimum number of components with no cross-validation. To obtain the statistical confidence limits on the analysis, PLS analysis using 100 bootstrap groups with the optimum number of components was performed. The PLS analysis with randomly interchanged biological activity was performed to estimate the extent of chance correlation.

Predictive r^2 Values. The predictive ability of each analysis was determined from a set of 10 compounds that were not included in the training set. These compounds were aligned, and their activities were predicted by each PLS analysis. The predictive r^2 (r^2_{pred}) value will be based on molecules of the test set only and is defined as

$$r^2_{pred} = (\text{SD} - \text{PRESS})/\text{SD}$$

where SD is the sum of the squared deviations between the biological activities of the test set and mean activity of the training set molecules and PRESS is sum of the squared deviation between predicted and actual activity values for every molecule in the test set.

Results and Discussion

The results of the CoMFA studies are summarized in Table 4. From this table it is evident that the CoMFA-derived QSAR shows a good cross-validated r^2 and therefore indicates a considerable predictive and correlative capacity of the models. Initial analysis of model A using alignment I yielded r^2_{cv} of 0.630 (6 pc) and a

Table 4. Summary of CoMFA Results

	model A		model B	
	alignment I	alignment II	alignment I	alignment II
r^2_{cv}	0.630	0.520	0.660	0.549
SEP	0.816	0.929	0.782	0.963
r^2 conventional	0.970	0.983	0.965	0.940
std error	0.230	0.177	0.251	0.314
no. of comp.	6	6	6	3
F value	175.347	299.881	146.869	182.474
P value	0.000	0.000	0.000	0.000
steric contrib	0.59	0.581	0.736	0.716
electrostatic contrib	0.41	0.419	0.264	0.284
$r^2_{pred(test\ 1)}$	0.854	0.859	0.836	0.728
$r^2_{pred(test\ 2)}$	0.751	0.789	0.742	0.693
r^2_{bs}[a]	0.987	0.993	0.983	0.947
SD[a]	0.005	0.004	0.008	0.015

[a] Results of bootstrapped analysis (100 samplings).

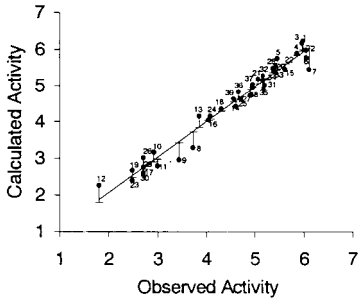

Figure 2. Calculated vs observed activity of the molecules of the training set for the CoMFA analysis of model B using alignment I; residuals are shown as error bars.

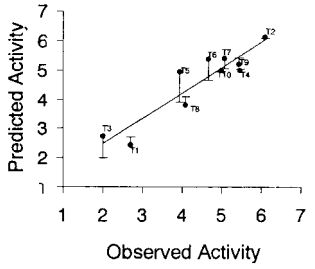

Figure 3. Predicted vs observed activity of the molecules of the test set for CoMFA analysis of model B using alignment I, residuals are shown as error bars.

conventional r^2 of 0.970. This analysis displayed a good predictive ability with $r^2_{pred(test\ 1)}$ of 0.854. A high bootstrapped (100 runs) r^2 of 0.987 ± 0.005 adds a high confidence limit to this analysis. Ionization of the P1 carboxylate (model B) seems to increase the internal consistency of the model with r^2_{cv} of 0.660 (6 pc) and a conventional r^2 of 0.965. The changes in steric and charge distributions due to ionization result in better representation of the data set. Figure 2 displays a plot of fitted vs observed activities of the molecules used in building a QSAR model, and the error bars depict the residuals. In this analysis both steric and electrostatic fields contribute to the QSAR equation by 73.6% and 26.4%, respectively, suggesting that variation in biological activity of inhibitors is dominated by differences in steric (van der Waals) interactions with the ICE active site. This analysis predicted the activities of the molecules of test set 1 with $r^2_{pred(test\ 1)}$ of 0.836. A graph depicting the plot of predicted vs observed activities of the test set can be found in Figure 3.

Realignment of the compounds using rigid body field fit (alignment II) decreased the significance of the

Table 5. Summary of CoMFA Results with Cross-validation by two Groups (Leave-Half-Out) and Randomized Biological Activities

	leave-half-out				randomization			
	model A		model B		model A		model B	
	I[a]	II[a]	I	II	I	II	I	II
mean r^2_{cv}[b]	0.531	0.470	0.552	0.456	−0.185	−0.218	−0.232	−0.229
SD[c]	0.093	0.073	0.078	0.077	0.156	0.158	0.189	0.194
highest r^2_{cv}	0.700	0.599	0.693	0.589	0.242	0.190	0.138	0.143
lowest r^2_{cv}	0.195	0.202	0.300	0.253	−0.541	−0.737	−0.834	−0.916

[a] Alignment I and II. [b] Mean of all 100 runs. [c] Standard deviation.

models. The analysis of model A yielded r^2_{cv} of 0.520 (6 pc) and a conventional r^2 of 0.983. This analysis displayed a good predictive ability with $r^2_{pred(test\ 1)}$ of 0.859. It was hoped that by realigning the charged molecules (model B) by rigid body field fit, the internal consistency of the model would improve. But the analysis of model B displayed a decreased r^2_{cv} of 0.549 and a conventional r^2 of 0.940. A respectable degree of predictability for the test set of molecules was produced with $r^2_{pred(test\ 1)}$ of 0.728.

The analyses using ionized ligands (model B) show high internal consistency as represented by cross-validated r^2 for both the alignments I and II. For both the models, better cross-validated and conventional r^2 values were obtained for alignment I as compared with alignment II. This illustrates the sensitivity of the CoMFA method to small changes in the orientation of the molecules. Since the alignments used in the present CoMFA study do not consider the entropic effects,[32] precise conclusions cannot be drawn regarding the binding modes of these ligands.

The leave-one-out cross-validation method might lead to high r^2_{cv} values which do not necessarily reflect a general predictiveness of the models. Therefore, we have performed cross-validation using two groups (leave-half-out). In this method 50% of the compounds were randomly selected and a model was generated, which was then used to predict the activity of the remaining 50% of compounds. The random formation of the cross-validation groups may have an effect on the results, hence cross-validation was performed 100 times for all the analysis. The mean r^2_{cv} values were reported in Table 5. The mean r^2_{cv} values were slightly lower compared to the values obtained with the leave-one-out method. In no case were r^2_{cv} values negative. The model B with alignment I had the highest mean r^2_{cv} value. The results obtained suggest that there is a good internal consistency in the underlying the data set.

The real test for model predictiveness is to predict the activity of ligands which were not used in the model generation. Our test set had 10 ligands which were randomly kept aside as a test set (test set 1). The CoMFA models exhibited a good predictiveness on these ligands. To further corroborate the predictiveness of the models we have predicted the activity of a set of 14 peptidomimetic ligands reported recently.[43] These 14 ligands (test set 2) were not known to us when we began this study. These ligands had benzoxapine acetamides, Freidinger lactam, bicyclic turned dipeptide (BTD), pipecolic acid, and pyridazinodiazepines as peptidomimetic surrogates (see Supporting Information). The activity of these ligands was predicted using the CoMFA

Table 6. Overlap of the CoMFA Contour Maps and ICE Active Site Residues

CoMFA regions	active site residues
1. sterically favored (green region)	Ala284 (LGB[b]),[a] Ile282 (LGB), Gln283 (LGB), Pro343 (P3[c]), Val348 (P4[d])
2. sterically unfavored (yellow region)	Ser332 (LGB), Val338 (P2[e]), Trp340 (P2), Arg341 (P3), His342 (P3)
3. positive charge favoring (blue region)	Cys285 (LGB), Gln283 (LGB), Ser332 (LGB), Gln385 (P3/P4)
4. negative charge favoring (red region)	Arg179 (P1[f]), Arg341 (P1/P3)

[a] Letters in parentheses indicate the site in ICE active site. [b] LGB = leaving group binding pocket. [c] P3 subsite. [d] P4 subsite. [e] P2 subsite. [f] P1 subsite.

models. A $r^2_{\text{pred(test 2)}}$ was calculated as stated earlier and is reported in Table 4. The $r^2_{\text{pred(test 2)}}$ values obtained suggest that the CoMFA models have good predictive ability.

The ICE inhibitors used in the present study act by forming a covalent bond with the Cys285 in which thiol group of Cys285 of ICE acts as a neucleophile and displaces the leaving group of the inhibitor in a S_N2 type reaction. To consider such interactions in CoMFA we have included lowest unoccupied molecular orbital (LUMO) energies of the inhibitors as a third regressor. The analysis of the QSAR data table shows that LUMO did not improve (data not shown) the statistical significance. Multiple regression analysis of LUMO energies with biological activity showed a r^2 of 0.030. Inclusion of ClogP,[44] a physicochemical parameter for lipophilicity, decreases the significance of the model (data not shown). It is apparent that the steric and electrostatic fields alone are adequate in CoMFA to characterize the variance in biological activity of these ICE inhibitors. A high bootstrap r^2 (100 runs) in all the analyses adds a high confidence limit to all the analyses. The correlations obtained were not based on chance correlations as can be seen from the cross-validated r^2 value (Table 5). All of the analyses were repeated 100 times with leave-one-out cross-validation each time after randomly interchanging the biological activities (random permutation testing) between the compounds. The means of the 100 runs are reported in Table 5. In all the analyses mean r^2_{cv} values were negative. This indicates greater than 99.9% likelihood that the relationship using correct assignment of the biological activities did not arise by chance.

To visualize the CoMFA steric and electrostatic fields from PLS analysis, contour maps of the product of the standard deviation associated with the CoMFA column and coefficient (SD × coeff) at each lattice point were generated. The contour maps are plotted as percentage contribution to the QSAR equation and are associated with the differences in biological activity. Though r^2_{cv} does not indicate a major difference in both the models, the CoMFA contour maps generated for model B do explain the structure−activity relationship of ICE inhibitors. Hence further interpretation of fields is based on the results obtained from alignment I of model B. In Figure 4A the regions of high and low steric tolerance are shown in green and yellow polyhedra, respectively. The areas of high steric bulk tolerance (80% contribution) are observed near P3 and P4 positions of the ligands. The active compound **2** shown in Figure 4A has valine and phenylalanine in these positions, respectively. The enhanced inhibitory activity shown by the compounds **1**−**7**, **15**, **20**−**22**, **28**, and **31**−**35** was due to the presence of bulky groups in the P3 and P4 positions surrounded by green contours in steric field plot. The steric map also shows the presence of a green contour in the vicinity of the leaving group of the inhibitors. This contour was observed in the bottom of leaving group binding pocket. The occupation of this area by a bulky group will have a positive effect on the biological activity as represented by compound **25,** which has more activity than compound **26** due to the presence of a bulky diphenylphosphinoxy leaving group. A wide range of residues are tolerated in the P2 subsite, but in the present study sterically unfavored yellow regions were observed near P2 subsite residue. The steric bulk in this region has a negative effect on the activity as represented by low activity of the compounds **17** (Figure 4A), **29**, and **30** that have a bulky phenyl or isobutyl substituent embedded in this yellow polyhedra. However, low activity of these compounds could be due to the absence of P1 aspartate residue. The CoMFA contour maps are consistent with the active site of ICE. The comparison of CoMFA contour plots and the active site of ICE should be viewed very carefully as CoMFA contour plots should not be overinterpreted as receptor maps.[17] The superimposition of CoMFA steric plots on active site residues is shown in Figure 4B. The overlapping residues of the ICE active site are given in Table 6. The sterically favorable green region was found to occupy the cavities in the enzyme, whereas the sterically unfavorable region overlaps with atoms of Val338, Trp340, Arg341, His342, and Ser332.

CoMFA electrostatic fields are shown as blue and red polyhedra in Figure 4C. A low electron density within the inhibitors near blue and red polyhedra, respectively, increases or decreases the activity. Though the electrostatic field contributions are less, a small change in electrostatic interactions will have a considerable effect on the activity. A predominant feature of the electrostatic field plot is the presence of a blue contour in the vicinity of the amide protons of P1 and P3 residue. Therefore, a low electron density in this area will have a positive effect on the biological activity. These protons are shown[15] to be involved in hydrogen-bonding interactions with the active site. The compounds **19** and **23** show low activity due to absence of free P1 or P3 amide protons. A blue contour was observed near the C-2 substituent of 5-amino pyrimidin-6-one system of the peptidomimetic inhibitors (Table 2). Therefore compounds with electron-withdrawing substituents on the C-2 carbon of 5-amino pyrimidin-6-one system show more activity (compound **31** vs **T10**). The blue contours were also observed near the leaving group, which coincide with the sterically favorable green contour observed at the bottom of the leaving group binding pocket. Therefore the leaving group of the inhibitors should have bulky substituents in the region of green contours, and it should also contain electron-withdrawing substituents. Such inhibitors can bind to ICE more tightly, and thus the electron-withdrawing substituent on the leaving group will reduce the electron density

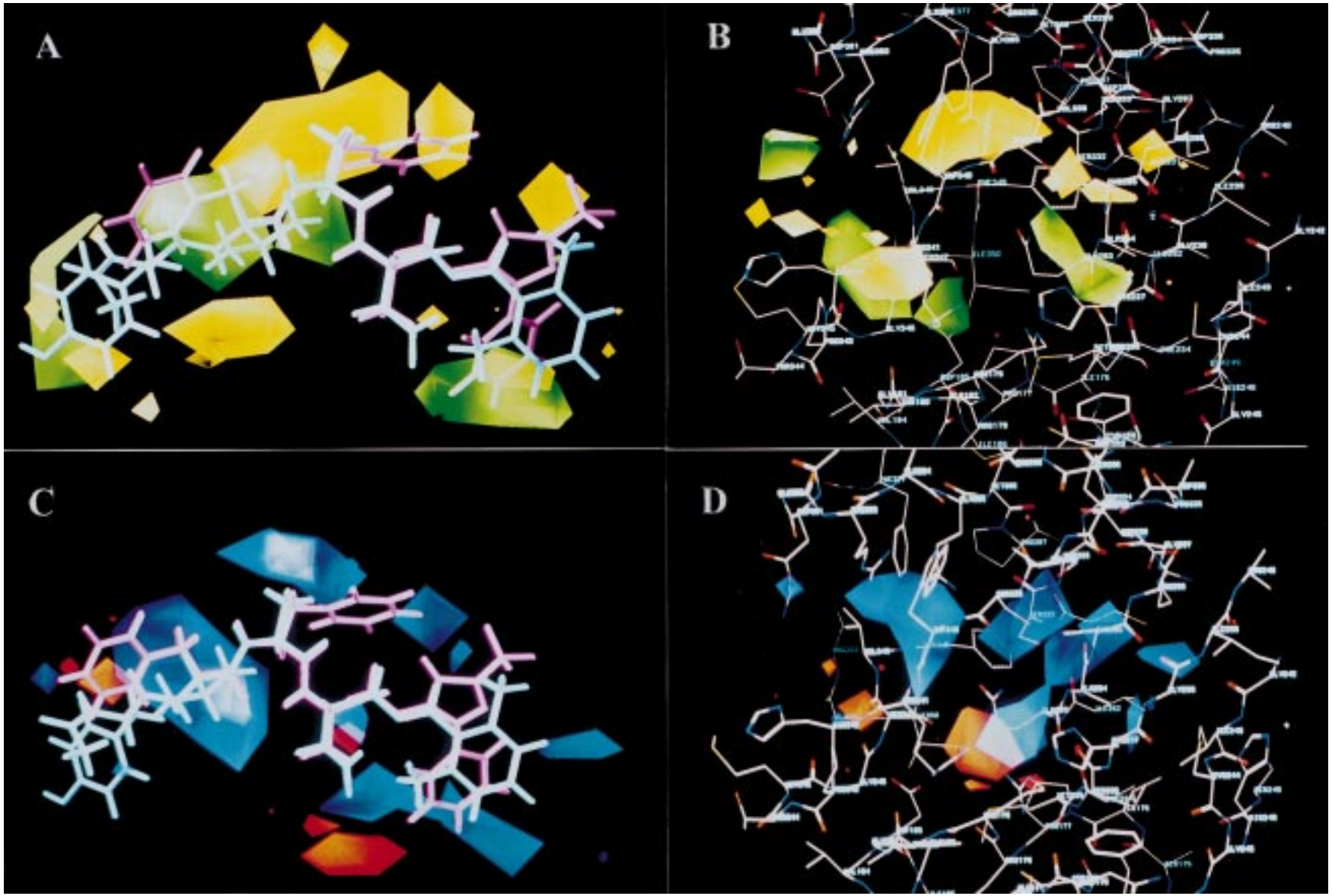

Figure 4. The CoMFA SD × coeff contour plots from the analysis of model B using alignment I. Steric contour plots: In panels A and B, favored (contribution level of 80%) and unfavored (contribution level of 20%) areas are represented as green and yellow contours, respectively. Electrostatic contour plots: In panels C and D, positive (contribution level of 80%) and negative (contribution level of 20%) charge favoring areas are represented as blue and red contours, respectively. In panels A and C, active compound **2** (cyan) and low active compound **17** (magenta) are shown, and in panels B and D, superimposition of steric and electorstatic contour plots on the active site of ICE are depicted.

around the methylene carbon of the methyl ketone moiety making it more vulnerable for neucleophilic attack. The intermolecular noncovalent interactions between the nonreacting part of the inhibitor and the active site of ICE may help to reduce the activation energy of the reaction between the enzyme and inhibitor. This suggests that the inherent structure of the inhibitor and leaving group is important for inhibition of ICE.

Very few high electron density favoring red regions were observed in the electrostatic field map (Figure 4C). A red polyhedra was observed near the P1 subsite. Compounds **17** (Figure 4C), **29Z**, **30**, and **1T** show poor activity since they lack P1 carboxylate which is essential for selectivity[9] and high activity. The superimposition of the electrostatic contour plot over the active site of ICE is shown in Figure 4D. Blue contours were observed near amino acid residues Cys285, Gln283, Ser332, Gln385 that are favorable to the positive charge (Table 6). Red contours were observed near Arg179 and Arg341 that favor negative charge.

Conclusions

We have derived a 3D-QSAR model using the CoMFA method to rationalize the ICE inhibitory activity of 49 compounds. The 3D-QSAR equation obtained using two alignment rules showed a high correlative and predictive ability. A high bootstrapped r^2 value and small standard deviations indicate that a similar relationship exists in all compounds. Negative values of the cross-validated r^2 in the randomization test reveal that the results were not based on chance correlation. Inclusion of LUMO energies that reflect the donor−acceptor interactions or ClogP, a lipophilicity parameter, did not improve the significance of the CoMFA models. Clearly, the steric and electrostatic fields of these compounds are adequate descriptors for structure−activity relationships. The CoMFA contour maps show a good compatibility with the receptor properties even though the conformations and alignments of the ligands were not based on the receptor structure. In the present study we have identified the importance of noncovalent interactions of these inhibitors. The leaving group of the compounds interacts in a hydrophobic pocket which protrudes from the surface of Cys285,[40] and such an interaction seems to play a significant role in the inactivation of ICE. This suggests that the inherent structure of the inhibitor as well as of the leaving group is important for biological activity. The structural requirements of the inhibitors identified through the CoMFA contour plots will help in designing new ICE inhibitors with enhanced activity.

Acknowledgment. We thank University Grants Commission (UGC) and All India Council for Technical Education (AICTE) for financial support to develop computer hardware and software facility. We also thank Drs. Dick Cramer and Allan Ferguson of Tripos Inc. USA, for critical reading of the manuscript. S.S.K. thanks Dr. Hariprasad, Mr. Tanaji, and Mr. Gokhale for useful discussions.

Supporting Information Available: A table of structures and activities of ICE inhibitors (test set 2) and a graph of predicted vs observed activity with residuals as error bars (4 pages). Ordering information is given in any current masthead page.

References

(1) Kostura, M. J.; Tocci, M. J.; Limjuco, G.; Chin, J.; Cameron, P.; Hillman, A. G.; Chartrain, N. A.; Schmidt, J. A. Indentification of a Monocyte Specific Pre-interleukin 1β Convertase Activity. *Proc. Natl. Acad. Sci. U.S.A.* **1989**, *86*, 5227−5231.

(2) Black, R. A.; Kronheim, S. R.; Sleath, P. R. Activation of Interleukin-1β by a Co-induced Protease. *FEBS Lett.* **1989**, *247*, 386-390.

(3) Thornberry, N. A.; Bull, H. G.; Calaycay, J. R.; Chapman, K. T.; Howard, A. D.; Kostura, M. J.; Miller, D. K.; Molineaux, S. M.; Weidner, J. R.; Aunins, J.; Elliston, K. O.; Ayala, J. A.; Casano, F. J.; Chin, J.; Ding, G. J.-F.; Egger, L. A.; Gaffney, E. P.; Limjuco, G.; Palyha, O. C.; Raju, S. M.; Rolando, A. M.; Salley, J. P.; Yamin, T. T.; Lee, T. D.; Shively, J. E.; MacCross, M.; Mumford, R. A.; Schmidt, J. A.; Tocci, M. J. A Novel Heterodimeric Cysteine Protease is Required for Interleukin-1β Processing in Monocytes. *Nature* **1992**, *356*, 768−774.

(4) Howard, A. D.; Kostura, M. J.; Thornberry, N.; Ding, G. J. F.; Limjuco, G.; Weidner, J.; Salley, J. P.; Hogquist, K. A.; Chaplin, D. D.; Mumford, R. A.; Schmidt, J. A.; Tocci, M. J. IL-1-Converting Enzyme Requires Aspartic Acid Residues for Processing of the IL-1β Precursor at Two Distinct Sites and Does Not Cleave 31-kDa IL-1α. *J. Immunol.* **1991**, *147*, 2964−2969.

(5) Dinarello, C. A.; Wolff, S. M. The Role of Interleukin-1 in Disease. *N. Engl. J. Med.* **1993**, *328*, 106−113.

(6) Hogquist, K. A.; Nett, M. A.; Unanue, E. R.; Chaplin, D. D. Interleukin 1 is Processed and Released During Apoptosis. *Proc. Natl. Acad. Sci. U.S.A.* **1991**, *88*, 8485−8469.

(7) Miura, M.; Zhu, H.; Rotello, R.; Hartwieg, E. A.; Yuan, J. Induction of Apoptosis in Fibroblasts by IL-1β-Converting Enzyme, A Mammalian Homologue of the C. elegans Cell Death Gene *ced-3*. *Cell* **1993**, *75*, 653−660.

(8) Barr. P. J.; Tomei, L. D. Apoptosis and its Role in Human Disease. *Biotechnology* **1994**, *12*, 487−493.

(9) Sleath, P. R.; Hendrickson, R. C.; Kronheim, S. R.; March, C. J.; Black, R. A. Substrate Specificity of the Protease That Processes Human Interleukin-1β. *J. Biol. Chem.* **1990**, *265*, 14526−14528.

(10) Chapman. K. T. Synthesis of a Potent, Reversible Inhibitor of Interleukin-1β Converting Enzyme. *Biorg. Med. Chem. Lett.* **1992**, *2*, 613−618.

(11) Graybill, T. L.; Dolle, R. E.; Helaszek, C. T.; Miller, R. E.; Ator, M. A. Preparation and Evaluation of Peptidic Aspartyl Hemiacetals as Reversible Inhibitors of Interleukin-1β Converting Enzyme (ICE). *Int. J. Peptide Protein Res.* **1994**, *44*, 173−182.

(12) Krantz, A.; Copp, L. J.; Coles, P. J.; Smith, R. A.; Heard, S. B. Peptidyl (Acyloxy)methyl Ketones and the Quiescent Affinity Label Concept: The Departing Group as a Variable Structural Element in the Design of Inactivators of Cysteine Proteinases. *Biochemistry* **1991**, *30*, 4678−4687.

(13) Thornberry, N. A.; Peterson, E. P.; Zhao, J. J.; Howard, A. D.; Griffin, P. R.; Chapman, K. T. Inactivation of Interleukin-1β Converting Enzyme by Peptide (Acyloxy)methyl Ketones. *Biochemistry* **1994**, *33*, 3934−3940.

(14) Dolle, R. E.; Hoyer, D.; Prasad, C. V. C.; Schmidt, S. J.; Helaszek, C. T.; Miller, R. E.; Ator, M. A. P1 Aspartate-Based Peptide α-((2,6-Dichlorobenzoyl)oxy)methyl Ketones as Potent Time-Dependent Inhibitors of Interleukin-1β-Converting Enzyme. *J. Med. Chem*, **1994**, *37*, 563−564.

(15) Dolle, R. E.; Singh, J.; Rinker, J.; Hoyer, D.; Prasad, C. V. C.; Graybill, T. L.; Salvino, J. M.; Helaszek, C. T.; Miller, R. E.; Ator, M. A. Aspartyl α-((1-Phenyl-3-(trifluoro-methyl)-pyrazol-5-yl)-oxy)methyl Ketones as Interleukin-1β Converting Enzyme Inhibitors. Significance of the P_1 and P_3 Amido Nitrogens for Enzyme-Peptide Inhibitor Binding. *J. Med. Chem.* **1994**, *37*, 3863−3866.

(16) Dolle, R. E.; Singh, J.; Whipple, D.; Osifo, I. K.; Speier, G.; Graybill, T. L.; Gregory, J. S.; Harris, A. L.; Helaszek, C. T.; Miller, R. E.; Ator, M. A. Aspartyl α-((Diphenyl-phosphinyl)oxy)-methyl Ketones as Novel Inhibitors of Interleukin-1β Converting Enzyme. Utility of the Diphenylphosphinic Acid Leaving Group for the Inhibition of Cysteine Proteases. *J. Med. Chem.* **1995**, *38*, 220−222.

(17) Cramer, R. D., III.; Patterson, D. E.; Bunce, J. D. Comparative Molecular Field Analysis (CoMFA). 1. Effect of Shape on Binding of Steroids to Carrier Proteins. *J. Am. Chem. Soc.* **1988**, *110*, 5959−5967.

(18) Clark, M.; Cramer, R. D., III; Jones, D. M.; Patterson, D. E.; Simeroth, P. E. Comparative Molecular Field Analysis (CoMFA) 2. Toward its use with 3-D structural Databases. *Tetrahedron Comput. Method* **1990**, *3*, 47−59.

(19) Wold, S.; Ruhe, A.; Wold, H.; Dunn, W. J. The Covariance Problem In Linear Regression. The Partial Least Squares (PLS) Approach to Generalized Inverses. *SIAM J. Sci. Stat. Comput.* **1984**, *5*, 735−743.
(20) Cramer, R. D., III, Bunce, J. D.; Patterson, D. E. Crossvalidation, Bootstrapping and Partial Least Squares Compared with Multiple Regression in Conventional QSAR Studies. *Quant. Struct.-Act. Relat.* **1988**, *7*, 18−25.
(21) Loughney, D. A.; Schwender, C. F. A Comparison of Progestin and Androgen Receptor Binding using the CoMFA Technique. *J. Comput.-Aided Mol. Des.* **1992**, *6*, 569−581.
(22) Bjorkroth, J. P.; Pakkanen, T. A.; Lindroos, J.; Pohjala, E.; Hanhijarvi, H.; Lauren, L.; Hannuniemi, R.; Juhakoski, A.; Kippo, K.; Kleimola, T. Comparative Molecular Field Analysis of Some Clodronic Acid Esters. *J. Med. Chem.* **1991**, *34*, 2338−2343.
(23) Raghavan, K.; Buolamwini, J. K.; Fesen, M. R.; Pommier, Y.; Kohn, K. W.; Weinstein, J. N. Three-Dimensional Quantitative Structure−Activity Relationship (QSAR) of HIV Integrase Inhibitors: A Comparative Molecular Field Analysis (CoMFA) Study. *J. Med. Chem.* **1995**, *38*, 890−897.
(24) DePriest, S. A.; Mayer, D.; Naylor, C. B.; Marshall, G. R. 3D-QSAR of Angiotensin-Converting Enzyme and Thermolysin Inhibitors: A Comparison of CoMFA Models Based on Deduced and Experimentally Determined Active Site Geometries. *J. Am. Chem. Soc.* **1993**, *113*, 5372−5384.
(25) Waller, C. L.; Marshall, G. R. Three-Dimensional Quantitative Structure−Activity Relatioship of Angiotensin-Converting Enzyme and Thermolysin Inhibitors. II. A Comparison of CoMFA Models Incorporating Molecular Orbital Fields and Desolvation Free Energies Based on Active-Analogue and Complementary-Receptor-Field Alignment Rules. *J. Med. Chem.* **1993**, *36*, 2390−2403.
(26) Horwitz, J. P.; Massova, I.; Wiese, T. E.; Wozniak, A. J.; Corbett, T. H.; Sebolt-Leopold, J. S.; Capps, D. B.; Leopold, W. R. Comparative Molecular Field Analysis of in Vitro Growth Inhibition of L1210 and HCT-8 Cells by Some Pyrazoloacridines. *J. Med. Chem.* **1993**, *36*, 3511−3516.
(27) Waller, C. L.; McKinney, J. D. Comparative Molecular Field Analysis of Polyhalogenated Dibenzo-*p*-dioxins, Dibenzofurans, and Biphenyls. *J. Med. Chem.* **1992**, *35*, 3660−3666.
(28) Tong, W.; Collantes, E. R.; Chen, Y.; Welsh, W. J. A Comparative Molecular Field Analysis Study of *N*-Benzylpiperidines as Acetylcholinesterase Inhibitors. *J. Med. Chem.* **1996**, *39*, 380−387.
(29) Cho, S. J.; Garsia, M. L. S.; Bier, J.; Tropsha, A. Structure-Based Alignment and Comparative Molecular Field Analysis of Acetylcholinesterase Inhibitors. *J. Med. Chem.* **1996**, *39*, 5064−5071.
(30) Waller, C. L.; Oprea, T. I.; Giolitti, A.; Marshall, G. R. Three-Dimensional QSAR of Human Immunodeficiency Virus (I) Protease Inhibitors. 1. A CoMFA Study Employing Experimentally-Determined Alignment Rules. *J. Med. Chem.* **1993**, *36*, 4152−4160.
(31) Diana, G. D.; Kowalczyk, P.; Treasurywala, A. M.; Oglesby, R. C.; Pevear, D. C.; Dutko, F. J. CoMFA Analysis of the Interactions of Antipicornavirus Compounds in the Binding Pocket of Human Rhinovirus-14. *J. Med. Chem.* **1992**, *35*, 1002−1008.
(32) Klebe, G.; Abraham, U. On the Prediction of Binding Properties of Drug Molecules by Comparative Molecular Field Analysis. *J. Med. Chem.* **1993**, *36*, 70−80.
(33) Nicklaus, M. C.; Milne, G. W. A.; Burke, T. R. Jr. QSAR of Conformationally Flexible Molecules. Comparative Molecular Field Analysis of Protein-Tyrosine Kinase Inhibitors. *J. Comput.-Aided Mol. Des.* **1992**, *6*, 487−504.
(34) Wilson, K. P.; Black, J. A.; Thomson, J. A.; Kim, E. E.; Griffith, J. P.; Navia, M. A.; Murcko, M. A.; Chambers, S. P.; Aldape, R. A.; Raybuck, S. A.; Livingston, D. J. Structure and Mechanism of Interleukin-1β Converting Enzyme. *Nature* **1994**, *370*, 270−275.
(35) Dolle, R. E.; Prouty, C. P.; Prasad, C. V. C.; Cook, E.; Saha, A.; Ross, T. M.; Salvino, J. M.; Helaszek, C. T.; Ator, M. A. First Examples of Peptidomimetic Inhibitors of Interleukin-1β Converting Enzyme. *J. Med. Chem.* **1996**, *39*, 2438−2440.
(36) SYBYL 6.22 molecular modelling software is available from Tripos Associates Inc., 1699 S. Hanley Road, St. Louis, MO 63144-2913.
(37) Clark, M.; Cramer, R. D., III; Van Opdenbosh, N. Validation of the General Purpose Tripos 5.2 Force Field. *J. Comput. Chem.* **1989**, 10, 982−1012.
(38) Dewar, M. J. S.; Zoebisch, E. G.; Healy, E. F.; Stewart, J. J. P. AM1 A New General Purpose Quantum Mechanical Molecular Model. *J. Am. Chem. Soc.* **1985**, *107*, 3902−3909.
(39) The program MOPAC 6.0 is available from Quantum Chemistry Program Exchange, no. 455.
(40) Hariprasad, V.; Kulkarni, V. M.; Docking of a Series of Peptide-Based Interleukin-1β Converting Enzyme Inhibitors with Aspartyl Hemiacetals, α-((2,6-Dichlorobenzoyl)oxy)methyl and (Acyloxy)methyl Ketone Moieties. *J. Mol. Model.* **1997**, *3*, 443−454.
(41) Walker, N. P. C.; Talanian, R. V.; Brady, K. D.; Dang, L. C.; Bump, N. J.; Ferenz, C. R.; Franklin, S.; Ghayur, T.; Hackett, M. C.; Hammill, L. D.; Herzog, L.; Hugunin, M.; Houy, W.; Mankovich, J. A.; McGuiness, L.; Oriewicz, E.; Paskind, M.; Pratt, C. A.; Reis, P.; Summani, A.; Terranova, M.; Welch, J. P.; Xiong, L.; Moller, A.; Tracey, D. E.; Kamen, R.; Wong, W. W. Crystal Structure of the Cysteine Protease Interleukin-1β-Converting Enzyme: A $(p20/p10)_2$ Homodimer. *Cell* **1994**, *78*, 343−352.
(42) *SYBYL 6.2 Theory Manual*; Tripos Associates: St. Louis, MO, July 1995; p 56.
(43) Dolle, R. E.; Prasad, C. V. C.; Prouty, C. P.; Salvino, J. M.; Awad, M. M. A.; Schmidt, S. J.; Hoyer, D.; Ross, T. M.; Graybill, T. L.; Speier, G. J.; Uhl, J.; Miller, B. E.; Helaszek, C. T.; Ator, M. A.; Pyridazinodiazepines as High-Affinity, P_2-P_3 Peptidomimetic Class of Interleukin − 1β-Converting Enzyme Inhibitor. *J. Med. Chem.* **1997**, *40*, 1941−1946.
(44) *ClogP*, version 1.0.0; Biobyte Corp., 201 West, 4th St., Suite 204, Claremont, CA 91711.

JM9708442